

Weak Ferromagnetism and Dynamic Magnetic Behavior of Two 2D Compounds with Hydroxy/Carboxylate-Bridged Co(II) Chains

Xiao-Ning Cheng, Wei Xue, Wei-Xiong Zhang, and Xiao-Ming Chen*

MOE Laboratory of Bioinorganic and Synthetic Chemistry, School of Chemistry and Chemical Engineering, Sun Yat-Sen University, Guangzhou 510275, China

Received May 8, 2008. Revised Manuscript Received June 24, 2008

Two isomorphous compounds $[A\text{Co}(\text{pa})(\text{OH})]_n$ ($\mathbf{1}\cdot\mathbf{K}$, $A = \text{K}$, and $\mathbf{1}\cdot\mathbf{Cs}$, $A = \text{Cs}$; H_2pa = phthalic acid) have been synthesized by solvothermal reaction of cobalt acetate, H_2pa , KOH solution, or Cs_2CO_3 in MeOH. Single-crystal X-ray diffraction shows that they both crystallize in the monoclinic space group $C2/c$ with small differences in the lattice parameters. Their structures are built up from Co^{II} zigzag chains, which are connected and separated by alkali metal ions and pa ligands to form two-dimensional layers. These layers are packed in ABAB fashion into a three-dimensional network by the π - π interactions. Both of them show spin canting behaviors, for the antisymmetric exchange between adjacent Co^{II} atoms in the chain, with the critical temperature $T_c = 7$ K for $\mathbf{1}\cdot\mathbf{K}$ and 6 K for $\mathbf{1}\cdot\mathbf{Cs}$. The magnetic coupling between Co^{II} atoms in them are estimated based on the model developed by Fisher for a uniform chain of classical spins with the best fit gives $J = -5.99$ cm $^{-1}$ for $\mathbf{1}\cdot\mathbf{K}$ and $J = -7.26$ cm $^{-1}$ for $\mathbf{1}\cdot\mathbf{Cs}$. At the same time, the noncritical-scaling theory is also used to reveal the ferrimagnetic-like behaviors of these two compounds. Moreover, dynamic magnetic relaxations are observed for these compounds, which are scarce for simple chains with uniform antiferromagnetic interactions.

Introduction

The design and synthesis of molecule-based magnets has been of considerable interest in recent years,¹ while the discovery and characterization of low-dimensional magnetic compounds, especially single-molecule magnets (SMMs) and single-chain magnets (SCMs) for their unusual physical properties and potential applications in quantum computing, is one of the most fascinating developments in this field.² Constructions of magnetic clusters and chains into extended networks are hoped to not only improve the quantum properties of the original units through certain cooperative effects mediated by covalent linkers but also provide a complete picture of dynamic variation straddling both quantum and classical regimes by modulating the intermolecular interactions.^{3,4} A series of one-dimensional (1D), 2D, and 3D compounds based on double-cuboidal Mn_4 SMMs have been obtained by bridging of N_3^- and $\text{N}(\text{CN})_2^-$, showing from SMM to classical magnet and dynamic behaviors.³ Recently, by using the σ -bond linkers as significantly weaker mediators of the spin carriers, 1D Ising

ferromagnetic chains were assembled into a 2D network to exhibit SCM behaviors.⁴

The magnetically inert alkali metal ions are also a good choice to tune the metal–ligand ratio for unique magnetic structures and to separate the magnetic interactions between spin carriers. A well-known example is the use of the diamagnetic ions to separate the magnetic Kagomé layers in the jarosite $\text{AFe}_3(\text{SO}_4)_2(\text{OH})_6$ ($A = \text{Na}^+$, K^+ , Rb^+ , Ag^+ , Ti^+ , NH_4^+ , H_3O^+ , $(1/2)\text{Pb}^{2+}$, or $(1/2)\text{Hg}^{2+}$).⁵ Moreover, the Winpenny and Powell groups have reported a few SMMs with unique structures by introducing alkali metal ions.⁶

Considering the hard/soft-acid/base principle, polycarboxylate ligands were chosen by us to catch alkali metal

* To whom correspondence should be addressed. E-mail: cxm@mail.sysu.edu.cn.

- (1) (a) Kahn, O. *Molecular Magnetism*; VCH: New York, 1993. (b) Kahn, O. *Adv. Inorg. Chem.* **1996**, *43*, 179. (c) Miller, J. S.; Epstein, A. J. *Angew. Chem., Int. Ed.* **1994**, *33*, 385. (d) Coronado, E.; Palacio, F.; Veciana, J. *Angew. Chem., Int. Ed.* **2003**, *42*, 2570.
- (2) (a) Sessoli, R.; Gatteschi, D.; Caneschi, A.; Novak, M. A. *Nature* **1993**, *365*, 141. (b) Gatteschi, D.; Sessoli, R. *Angew. Chem., Int. Ed.* **2003**, *43*, 268. (c) Caneschi, A.; Gatteschi, D.; Lalioti, N.; Sangregorio, C.; Sessoli, R.; Venturi, G.; Vindigni, A.; Rettori, A.; Pini, M. G.; Novak, M. A. *Angew. Chem., Int. Ed.* **2001**, *40*, 1760. (d) Clérac, R.; Miyasaka, H.; Yamashita, M.; Coulon, C. *J. Am. Chem. Soc.* **2002**, *124*, 12837. (e) Liu, T.-F.; Fu, D.; Gao, S.; Zhang, Y.-Z.; Sun, H.-L.; Su, G.; Liu, Y.-J. *J. Am. Chem. Soc.* **2003**, *125*, 13976. (f) Wang, S.; Zuo, J.-L.; Gao, S.; Zhou, H.-C.; Zhang, Y.-Z.; You, X.-Z. *J. Am. Chem. Soc.* **2004**, *126*, 8900.

- (3) (a) Clérac, R.; Miyasaka, H.; Yamashita, M.; Coulon, C. *J. Am. Chem. Soc.* **2002**, *124*, 12837. (b) Miyasaka, H.; Nakata, K.; Sugiura, K.-i.; Yamashita, M.; Clérac, R. *Angew. Chem., Int. Ed.* **2004**, *43*, 707. (c) Miyasaka, H.; Nakata, K.; Lecren, L.; Coulon, C.; Nakazawa, Y.; Fujisaki, T.; Sugiura, K.-i.; Yamashita, M.; Clérac, R. *J. Am. Chem. Soc.* **2006**, *128*, 3770. (d) Miyasaka, H.; Yamashita, M. *Dalton Trans.* **2007**, 399.
- (4) (a) Zheng, Y.-Z.; Tong, M.-L.; Zhang, W.-X.; Chen, X.-M. *Angew. Chem., Int. Ed.* **2006**, *45*, 6310. (b) Zheng, Y.-Z.; Xue, W.; Tong, M.-L.; Chen, X.-M.; Grandjean, F.; Long, G. J. *Inorg. Chem.* **2008**, *47*, 4077.
- (5) (a) Nocera, D. G.; Bartlett, B. M.; Grohol, D.; Papoutsakis, D.; Shores, M. P. *Chem. Eur. J.* **2004**, *10*, 3850. (b) Grohol, D.; Matan, K.; Lee, J.-H.; Lynn, J. W.; Nocera, D. G.; Lee, Y. S. *Nat. Mater.* **2005**, *4*, 323. (c) Paul, G.; Choudhury, A.; Sampathkumaran, E. V.; Rao, C. N. R. *Angew. Chem., Int. Ed.* **2002**, *41*, 4297. (d) Rao, C. N. R.; Sampathkumaran, E. V.; Nagarajan, R.; Paul, G.; Behera, J. N.; Choudhury, A. *Chem. Mater.* **2004**, *16*, 1441.
- (6) (a) Schmitt, W.; Hill, J. P.; Juanico, M. P.; Caneschi, A.; Costantino, F.; Anson, C. E.; Powell, A. K. *Angew. Chem., Int. Ed.* **2005**, *44*, 4187. (b) Schmitt, W.; Hill, J. P.; Malik, S.; Volkert, C. A.; Ichinose, I.; Anson, C. E.; Powell, A. K. *Angew. Chem., Int. Ed.* **2005**, *44*, 7048. (c) Brechin, E. K.; Gould, R. O.; Harris, S. T.; Parsons, S.; Winpenny, R. E. P. *J. Am. Chem. Soc.* **1996**, *118*, 11293. (d) Aromí, G.; Roubeau, O.; Helliwell, M.; Teat, S. J.; Winpenny, R. E. P. *Dalton Trans.* **2003**, 3436.

ions and to separate spin carriers. Mixed hydroxy/carboxylate-bridged Co^{II} Δ -chains were embedded in a 3D network using 4-carboxyl-phenoxy-acetate as ligand by us, in which the Δ -chains are well divided by organic ligands and Na^+ ions, showing a SCM-like behavior.⁷ As a sequel to that work, we report herein two new 2D coordination polymers $[\text{A}(\text{Co}(\text{pa})(\text{OH}))_n]_n$ (**1**·**K**, A = K, and **1**·**Cs**, A = Cs, H_2pa = phthalic acid) consisting of mixed hydroxy/carboxylate-bridged Co^{II} zigzag chains separated by alkali metals and organic pa ligands, which exhibit weak ferromagnetic behavior and slow magnetic relaxations.

Experimental Section

Materials and Physical Measurements. All solvents and starting materials for synthesis were purchased commercially and used as received. Infrared spectra were obtained from KBr pellets on a Bruker TENSOR 27 Fourier transform infrared spectrometer in the 400–4000 cm^{-1} region. Elemental analyses (C, H, N) were performed on a Perkin-Elmer 240 elemental analyzer. Powder X-ray diffraction (PXRD) data were recorded on a Rigaku D/M-2200T automated diffractometer.

All ac and dc magnetic data were collected on a Quantum Design MPMS XL-7-SQUID magnetometer with phase-pure samples from crushed single crystals (Figure S1, Supporting Information), in which the ac susceptibility measurements were performed at frequencies between 1 and 1000 Hz with an ac field of 0.0005 T and with a zero or 0.1 T applied dc field. The powder samples of **1**·**K** and **1**·**Cs** were embedded in grease to avoid any field induced crystal reorientation. A diamagnetic correction of $-1.8 \times 10^{-4} \text{ cm}^3 \text{ mol}^{-1}$ was calculated from Pascal constants and applied to the observed magnetic susceptibility of **1**·**K** and **1**·**Cs**.

Synthesis of $[\text{KCo}(\text{pa})(\text{OH})]_n$ (1**·**K**).** Reaction of a mixture of H_2pa (0.08 g, 0.5 mmol), $\text{Co}(\text{OAc})_2 \cdot 4\text{H}_2\text{O}$ (0.150 g, 0.6 mmol), an aqueous solution of KOH (2 M, 8 drops), and methanol (12 mL) in a 15 mL Teflon lined bomb at 160 °C for 3 days afforded green sheet-like crystals (yield ca. 62%). Anal. Calcd (%) for $\text{C}_8\text{H}_5\text{CoKO}_5$: C, 34.42; H, 1.81. Found: C, 34.40; H, 1.85. IR (KBr, cm^{-1}): 3651w, 3058w, 1608m, 1557vs, 1492w, 1419s, 1387s, 1148w, 1074w, 855w, 824m, 818s, 731m, 677m, 584w, 494w, 443w.

Synthesis of $[\text{CsCo}(\text{pa})(\text{OH})]_n$ (1**·**Cs**).** **1**·**Cs** was synthesized analogously to **1**·**K** by using Cs_2CO_3 (0.147 g, 0.45 mmol) in place of the solution of KOH. The yield was approximately 57%. Anal. Calcd (%) for $\text{C}_8\text{H}_5\text{CoCsO}_5$: C, 25.76; H, 1.35. Found: C, 25.73; H, 1.36. IR (KBr, cm^{-1}): 3656 (w), 1617(m), 1568(s), 1483(w), 1410(s), 1387(s), 1142(w), 853(m), 828(m), 793(s), 739(m), 691(m), 654(w), 508(w), 447(w).

X-ray Crystallography. Single-crystal X-ray diffraction measurements of **1**·**K** and **1**·**Cs** were carried out on a Bruker Smart APEX CCD area-detector diffractometer (Mo $\text{K}\alpha$, 0.71073 Å) at 293(2) K. Absorption corrections were applied by using the multiscan program SADABS. The structures were solved with direct methods and refined with a full-matrix least-squares technique with the SHELXTL program package.⁸ All non-hydrogen atoms were refined with anisotropic displacement parameters. The organic hydrogen atoms were generated geometrically (C–H, 0.96 Å). Crystal data and details of data collections and refinement for **1**·**K** and **1**·**Cs** are summarized in Table 1. The selected bond lengths

Table 1. Crystallographic Data and Refinement Parameters for **1·**K** and **1**·**Cs**^a**

| | 1 · K | 1 · Cs |
|---|-------------------------------------|--------------------------------------|
| formula | $\text{CoKC}_8\text{H}_5\text{O}_5$ | $\text{CoCsC}_8\text{H}_5\text{O}_5$ |
| fw | 279.15 | 372.96 |
| <i>T</i> , K | 298 | 298 |
| crystal system | monoclinic | monoclinic |
| space group | <i>C2/c</i> | <i>C2/c</i> |
| <i>a</i> , Å | 20.638(2) | 20.680(5) |
| <i>b</i> , Å | 6.5041(7) | 6.634(2) |
| <i>c</i> , Å | 13.437(1) | 13.909(4) |
| β , deg | 94.150(2) | 92.946(4) |
| <i>V</i> , Å ³ | 1798.9(3) | 1905.7(8) |
| <i>Z</i> | 8 | 8 |
| <i>D_c</i> , g cm ⁻³ | 2.061 | 2.600 |
| μ , mm ⁻¹ | 2.365 | 5.561 |
| unique reflns/ <i>R</i> _{int} | 1683/0.0220 | 1732/0.0266 |
| <i>R</i> ₁ (<i>I</i> > 2 θ) | 0.0303 | 0.0576 |
| <i>wR</i> ₂ (all data) | 0.0789 | 0.1366 |
| GO ^F | 1.038 | 1.136 |
| $\Delta\rho_{\text{min/max}}$ (e/Å ³) | -0.462/0.418 | -1.332/ 2.594 |

$$^a R_1 = \sum |F_o| - |F_c| / \sum |F_o|, wR_2 = [\sum w(F_o^2 - F_c^2)^2 / \sum w(F_o^2)^2]^{1/2}.$$

and bond angles of **1**·**K** and **1**·**Cs** are listed in Table S1, Supporting Information.

Results and Discussion

Crystal Structures. X-ray analysis reveals that the asymmetric unit of **1**·**K** contains two Co^{II} atoms at special positions (Co1 is at a mirror plane, while Co2 occupies an inversion center), one K^+ ion at a general position, one pa ligand, and one hydroxy group (Figure 1a). Each Co^{II} atom is surrounded by four carboxylate oxygen atoms from four different pa ligands and two hydroxy groups, furnishing a distorted octahedral geometry (Co1–O, 1.986–2.219 Å; Co2–O, 1.973–2.225 Å). The K^+ ion is also in a distorted octahedral geometry with one hydroxy group and five carboxylate oxygen atoms from three different pa ligands (K1–O, 2.704–2.988 Å). The hydroxy group acts as a μ_3 -bridge to ligate two Co^{II} atoms and one K^+ ion, while the pa ligand adopts a complicated mode as shown in Figure 1b. Each pair of Co^{II} atoms are bridged by two syn–syn carboxylate groups from two different pa ligands and one hydroxyl group into a 1D chain of corner-sharing octahedra that propagate in a zigzag fashion along the *c*-axis. The shortest intrachain $\text{Co}^{\text{II}} \cdots \text{Co}^{\text{II}}$ distance and Co1–O–Co2 angle are 3.39 Å and 117.7°, respectively. Adjacent chains are interlinked into layers by pa ligands with the shortest interchain $\text{Co}^{\text{II}} \cdots \text{Co}^{\text{II}}$ distance 6.50 Å in the *b*-direction. The K^+ ions are filled in the layers between the chains. Thus, isolated by K^+ ions and organic linkers, magnetic Co^{II} chains are constructed into the 2D layer (Figure 1c). These layers are packed in ABAB fashion along the *a*-axis into a 3D network through intermolecular π – π stacking interactions between the phenyl rings with a shortest interlayer $\text{Co}^{\text{II}} \cdots \text{Co}^{\text{II}}$ distance of approximately 10.82 Å (Figure S2, Supporting Information).

1·**Cs** is isomorphic with **1**·**K**. Since the radius of Cs^+ is larger than that of K^+ ion, there are a few distinct changes on the distances and angles. The Co^{II} atoms are still in the similar octahedra with slightly changed Co1–O (2.006–2.212 Å) and Co2–O (1.975–2.247 Å) bond lengths, while the Cs–O bonds (2.976 to 3.116 Å) are longer than the K–O

(7) Cheng, X.-N.; Zhang, W.-X.; Zheng, Y.-Z.; Chen, X.-M. *Chem. Commun.* **2006**, 3603.

(8) *SHELXTL 6.10*; Bruker Analytical Instrumentation: Madison, WI, 2000.

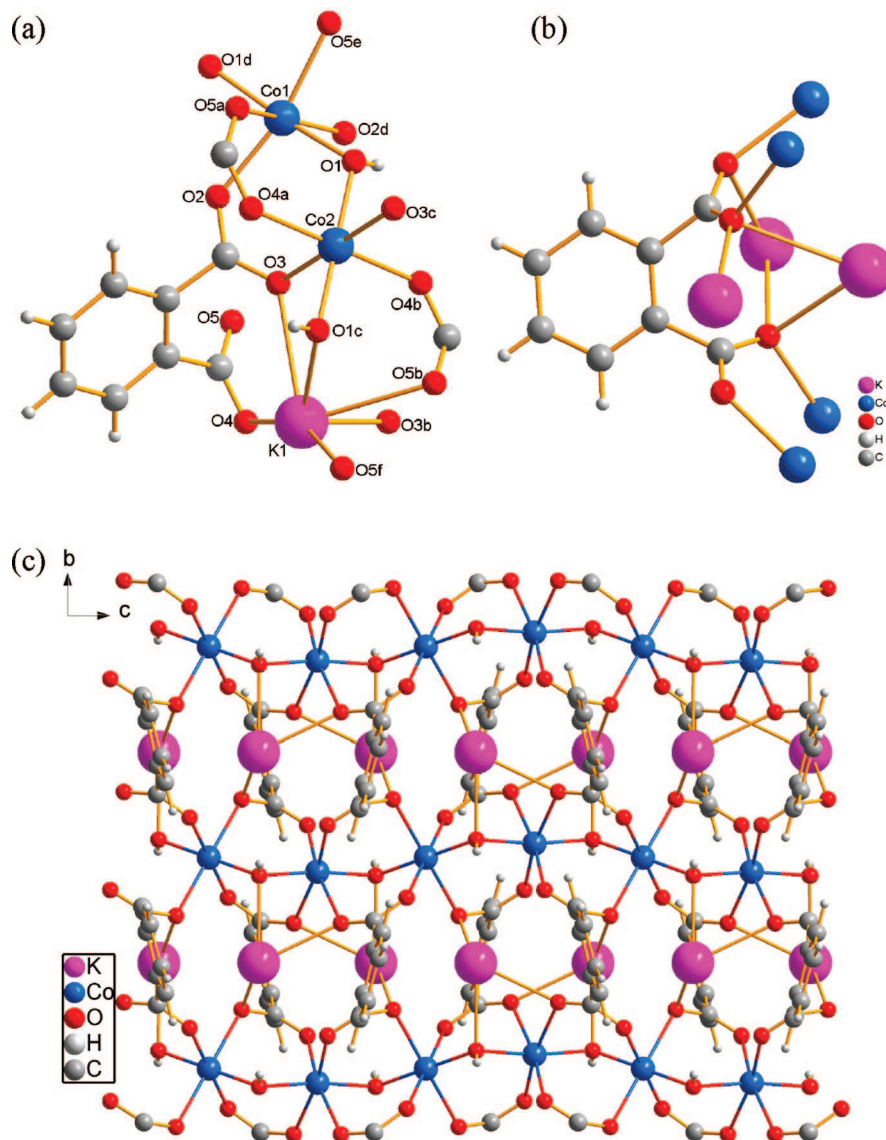


Figure 1. Coordination environments of Co(II) (a), coordination mode of pa ligand (b), and layer structure (c) in $1 \cdot \text{K}$. Symmetry codes: (a) $x, y + 1, z$; (b) $-x, -y - 1, -z + 1$; (c) $-x, -y, -z + 1$; (d) $-x, y, -z + 1/2$; (e) $-x, y + 1, -z + 1/2$; and (f) $x, -y - 1, z + 1/2$.

ones in $1 \cdot \text{K}$. In particular, the adjacent $\text{Co}^{\text{II}} \cdots \text{Co}^{\text{II}}$ distance and the $\text{Co1}-\text{O}-\text{Co2}$ bond angle in the chain in $1 \cdot \text{Cs}$, being sensitive to the magnetic properties, are 3.50 \AA and 122.8° , respectively, which are both slightly larger than those in $1 \cdot \text{K}$. Moreover, the shortest interchain and interlayer $\text{Co}^{\text{II}} \cdots \text{Co}^{\text{II}}$ distances in $1 \cdot \text{Cs}$ are 6.63 and 10.85 \AA , respectively.

Magnetic Properties. The magnetic properties of $1 \cdot \text{K}$ and $1 \cdot \text{Cs}$ are similar owing to their analogous structures. The temperature dependences of $\chi_{\text{M}}T$ for $1 \cdot \text{K}$ and $1 \cdot \text{Cs}$ at an applied field of 1 kOe are shown in Figures 2 and S5 (Supporting Information). The value of $\chi_{\text{M}}T$ for per Co^{II} at 300 K is $2.79 \text{ cm}^3 \text{ mol}^{-1} \text{ K}$ for $1 \cdot \text{K}$ and $2.97 \text{ cm}^3 \text{ mol}^{-1} \text{ K}$ for $1 \cdot \text{Cs}$, and the effective magnetic moments μ_{eff} are $4.72 \mu_{\text{B}}$ and $4.87 \mu_{\text{B}}$, respectively. They are slightly higher than the spin-only value resulting from the orbital contribution of the octahedral Co^{II} ions and typical for the octahedral complexes having the moment of $4.7\text{--}5.2 \mu_{\text{B}}$.⁹ As the temperature decreases, the $\chi_{\text{M}}T$ of $1 \cdot \text{K}$ decreases smoothly

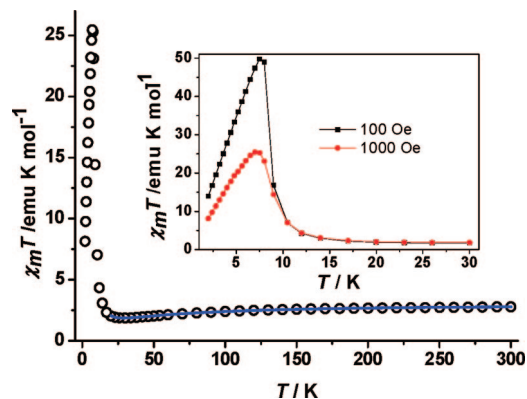


Figure 2. Temperature dependence of magnetic susceptibility of $1 \cdot \text{K}$, the line represents the best fit of the data by using eq 2. Inset: field-cooled (FC) magnetizations.

to a rounded minimum of $1.88 \text{ cm}^3 \text{ mol}^{-1} \text{ K}$ at about 30 K , then rises abruptly to a sharp maximum of $25.5 \text{ cm}^3 \text{ mol}^{-1} \text{ K}$ at about 11 K , and finally drops rapidly upon further cooling to 2 K . This behavior is reminiscent of a ferrimagnet

(9) Carlin, R. L. *Magnetochemistry*; Springer-Verlag: New York, 1981; p 117.

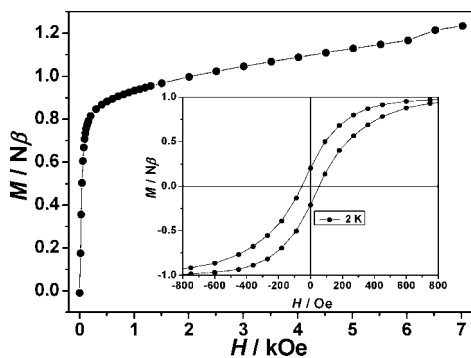


Figure 3. Field dependence of magnetization and hysteresis loop of $1\cdot\mathbf{K}$ at 2 K.

or a system of spin-canting.¹⁰ The shape of the magnetization curve for $1\cdot\mathbf{Cs}$ is uniform with that of $1\cdot\mathbf{K}$. Between 70 and 300 K, the magnetic susceptibility data of $1\cdot\mathbf{K}$ obey the Curie–Weiss law with Curie constant $C = 3.18 \text{ cm}^3 \text{ mol}^{-1} \text{ K}$ and Weiss constant $\theta = -30.1 \text{ K}$. The C value corresponds to $g = 2.60$, being normal for an octahedral Co^{II} , and the large negative value of the Weiss constant confirms the dominant exchange to be antiferromagnetic in $1\cdot\mathbf{K}$. In the case of $1\cdot\mathbf{Cs}$, $C = 3.28 \text{ cm}^3 \text{ mol}^{-1} \text{ K}$, $\theta = -31.0 \text{ K}$, and $g = 2.65$, which are all similar with those of $1\cdot\mathbf{K}$.

Considering the isolated 1D uniform chain structures in $1\cdot\mathbf{K}$ and $1\cdot\mathbf{Cs}$, eq 1, derived by Fisher for a uniform chain of classical spins based on the Hamiltonian $H = -J\sum S_i S_{i+1}$, was used to evaluate the antiferromagnetic interaction (J) of the neighboring Co^{II} bridged by two syn–syn carboxylate and one hydroxy groups.¹¹

$$\chi_{\text{chain}} = [Ng^2\beta^2 S(S+1)/(3kT)][(1+u)/(1-u)] \quad (1)$$

where u is the well-known Langevin function defined as $u = \coth[JS(S+1)/kT] - kT/[JS(S+1)]$ with $S = 3/2$ ($J > 0$ for ferromagnetic and $J < 0$ for antiferromagnetic coupling). The best least-squares fit of the experimental data $\chi_{\text{M}}T$ above 80 K to the above expressions led to $J = -5.99 \text{ cm}^{-1}$, $g = 2.53$, and $R = 6.24 \times 10^{-5}$ for $1\cdot\mathbf{K}$ (Figure S3, Supporting Information) and $J = -7.26 \text{ cm}^{-1}$, $g = 2.63$, and $R = 1.01 \times 10^{-5}$ for $1\cdot\mathbf{Cs}$, where $R = \sum(\chi_{\text{M}}T_{\text{cal}} - \chi_{\text{M}}T_{\text{obs}})^2/(\chi_{\text{M}}T_{\text{obs}})^2$ (Figure S6, Supporting Information). However, it should be noted that the results only imply stronger antiferromagnetic exchanges between metal ions in $1\cdot\mathbf{K}$ and those in $1\cdot\mathbf{Cs}$, while an exact estimation of the magnetic interactions is still unrealizable due to the orbital contribution in Co^{II} systems.

To investigate the ferrimagnetic-like behavior, where the $\chi_{\text{M}}T$ – T curves rise abruptly at the low temperature for $1\cdot\mathbf{K}$ and $1\cdot\mathbf{Cs}$, the noncritical-scaling theory with the following

simple phenomenological eq 2 was used to fit the experimental data from 300 to 20 K:¹²

$$\chi_{\text{M}}T = A \exp(-E_1/kT) + B \exp(-E_2/kT) \quad (2)$$

Here, the sum of A and B is merely the high-temperature Curie constant for one Co^{II} ion per formula, and $E_1 > 0$ indicates the antiferromagnetic interaction within the chain, which is responsible for the initial high temperature decay of $\chi_{\text{M}}T$. The low-temperature behavior, increasing of $\chi_{\text{M}}T$ below 25 K, is denoted by the second term with $E_2 < 0$ which is ferromagnetic-like. The best fit gives $A = 2.5$, $B = 0.5$, $E_1 = 25.0 \text{ cm}^{-1}$, and $E_2 = -16.1 \text{ cm}^{-1}$ for $1\cdot\mathbf{K}$ (Figure 2) and $A = 2.2$, $B = 1.1$, $E_1 = 38 \text{ cm}^{-1}$, and $E_2 = -7.4 \text{ cm}^{-1}$ for $1\cdot\mathbf{Cs}$ (Figure S7, Supporting Information), which suggest the coexistence of ferromagnetic and antiferromagnetic interactions and the dominant exchange to be antiferromagnetic.

To further investigate the phase transformation at low temperature, the field-cooled (FC) and zero-field-cooled (ZFC) magnetization measurements were performed for $1\cdot\mathbf{K}$ and $1\cdot\mathbf{Cs}$ at 20 Oe in the 2–30 K [Figures S5 and S8 (inset), Supporting Information]. Below 13 K, the FC curve of $1\cdot\mathbf{K}$ shows an abrupt increase with decreasing temperature, reaching saturation at lower T values, while the ZFC curve exhibits a rounded maximum and falls down below $T = 3.5 \text{ K}$. The FC and ZFC data are divergent below the critical temperature $T_c = 7 \text{ K}$, which indicates a possible transition from a paramagnetic state to either a long-range ordered, a spin-glass, or a superparamagnetic state.¹³ The FC and ZFC magnetization measurements also show a divergent below the critical temperature $T_c = 6 \text{ K}$. Moreover, FC magnetizations of $1\cdot\mathbf{K}$ and $1\cdot\mathbf{Cs}$ were measured under different applied fields. The magnetic behaviors are quite field-dependent, in which the rises of the $\chi_{\text{M}}T$ values at low temperature become less pronounced at higher fields (Figures 2 (inset) and S8, Supporting Information). This is an important feature of spin-canting behavior.¹⁰

The field-dependence of magnetization of $1\cdot\mathbf{K}$ and $1\cdot\mathbf{Cs}$ was also studied at different temperatures. The magnetization curve for $1\cdot\mathbf{K}$ of 2 K exhibits a sharp increase of the magnetization in the low-field region ($H < 2 \text{ kOe}$), and then, the magnetization increases slowly and linearly with the field (Figure 3). Finally, the magnetization value $1.37 \text{ N}\beta$ achieved at the highest field investigated (7 T) is far below the saturation value ($3 \text{ N}\beta$) expected for spin-only Co^{II} species. The same shape is also observed in the isothermal magnetization curve of $1\cdot\mathbf{Cs}$ at 2 K. These features support the coexistence of ferromagnetic and antiferromagnetic interactions in $1\cdot\mathbf{K}$ and $1\cdot\mathbf{Cs}$. The magnetization curves at other different temperatures below 10 K are all similar to that of 2 K. As the temperature further increases, the magnetic responses for $1\cdot\mathbf{K}$ and $1\cdot\mathbf{Cs}$ become weaker and weaker, even approaching the paramagnetic state (defined by Brillouin function with different parameters in Figures S4 and

(10) (a) Wang, X.-Y.; Wei, H.-Y.; Wang, Z.-M.; Chen, Z.-D.; Gao, S. *Inorg. Chem.* **2005**, *44*, 572. (b) Sun, H.-L.; Gao, S.; Ma, B.-Q.; Su, G. *Inorg. Chem.* **2000**, *42*, 5399. (c) Brechin, E. K.; Cador, O.; Caneschi, A.; Cadiou, C.; Harris, S. G.; Parsons, S.; Vonci, M.; Winpenny, R. E. P. *Chem. Commun.* **2002**, 1860. (d) Escuer, A.; Cano, J.; Goher, M. A. S.; Journaux, Y.; Lloret, F.; Mautner, F. A.; Vicente, R. *Inorg. Chem.* **2000**, *39*, 4688. (e) Cheng, L.; Zhang, W.-X.; Ye, B.-H.; Lin, J.-B.; Chen, X.-M. *Eur. J. Inorg. Chem.* **2007**, 2668.

(11) Fisher, M. E. *Am. J. Phys.* **1964**, *32*, 343.

(12) (a) *Magnetism: Molecules to Materials*; Miller, J. S., Drillon, M., Eds.; Wiley-VCH: Weinheim, Germany, 2005; Vol. 5, Chapter 10, p 347. (b) Drillon, M.; Panissod, P.; Rabu, P.; Souletie, J.; Ksenofontov, V.; Gütllich, P. *Phys. Rev. B: Condens. Matter Mater. Phys.* **2002**, *65*, 104404.

(13) Chernova, N. A.; Song, Y.-N.; Zavalij, P. Y.; Whittingham, M. S. *Phys. Rev. B* **2004**, *70*, 144405.

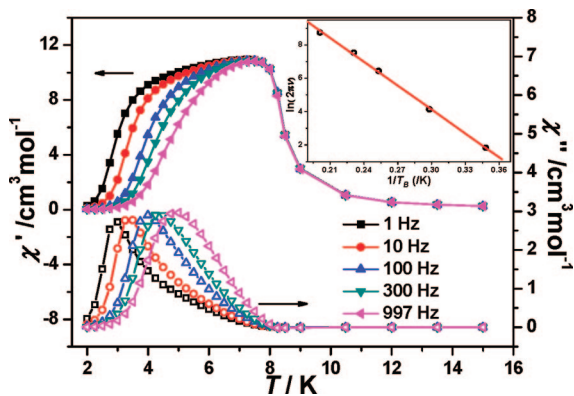


Figure 4. Frequency dependence of the ac susceptibility for **1·K**. Inset: the linear fit of the experimental data to the Arrhenius law.

S10, Supporting Information). Upon the demagnetization process, a small hysteresis is observed at 2 K with the remanent magnetization $M_r = 0.2 N\beta$ and the coercive field $H_c = 60$ Oe (Figure 3 inset). The shape and temperature dependence changes of magnetization curve for **1·Cs** are all similar with those of **1·K**. However, the hysteresis loop of **1·Cs** is smaller than that of **1·K**, even overlapping near the zero field.

Since the set of dc measurements does not provide enough evidence to distinguish between a magnetic order phase and a glassy behavior, the temperature dependence of real χ' and imaginary χ'' parts of ac susceptibility of **1·K** was then measured in an ac driving field of 5 Oe at different frequencies (Figure 4). Below 8.5 K, the real part χ' exhibits the Hopkinson maximum and then decreases in two steps on further cooling. In an ac field oscillating at a frequency of 1 Hz, the first step lies in the 8–4 K temperature range, where χ' diminishes smoothly and reaches an inflection point at $T_i = 4$ K. Below 4 K, the in-phase component cancels out very rapidly, in parallel with the abrupt decrease observed in the ZFC magnetization measurement. Below 8 K, χ'' increases steadily to reach a maximum and then vanishes very abruptly. Both χ' and χ'' shift toward higher temperatures as the frequency becomes higher. The shift of the peak temperature (T_p) of χ'' is measured by a parameter $\phi = \Delta T_p / [T_p \Delta(\log f)] = 0.13$, being larger than that for a canonical spin glass and closer to a normal value for a superparamagnet.¹⁴ The relaxation time was obtained from the Arrhenius law $\tau(T) = \tau_0 \exp(-\Delta/k_B T)$, and the best set of parameters are $\tau_0 = 9.24 \times 10^{-9}$ s and $\Delta/k_B = 48$ K [Figure 4 (inset)], suggesting a thermally activated mechanism. The τ_0 value is close to that expected for the relaxation time of octahedral Co^{II} centers.¹⁵ In the ac data of **1·Cs**, the frequency-dependent behaviors attend below 6.2 K, and the parameter ϕ measuring the shift of peak temperature is 0.11. The relaxation time $\tau_0 = 1.40 \times 10^{-10}$ s and energy gap $\Delta/k_B = 54$ K calculated by Arrhenius law are obtained for **1·Cs**, which are all similar to those of **1·K** (Figure S11, Supporting Information).

The most important structural feature of **1·Cs** and **1·K** is the uniform chain with carboxylate and hydroxyl groups as antiferromagnetic bridges. The chains are well separated by alkali metal ions K^+ or Cs^+ and pa ligands, which provide good examples on studying the magnetic behaviors of chains. The antiferromagnetic interactions tend to align the Co^{II} spins within the chain in a quits (counteracting) way to give a zero residual moment, but the low-temperature magnetic behaviors suggest the existence of uncompensated residual moments and the occurrence of weak ferromagnetic ordering. It is well-known that spin canting may arise from single-ion magnetic anisotropy and/or antisymmetric exchange (Dzyaloshinsky–Moriya interaction). In these compounds, although the zigzag chain is centrosymmetric with Co^{II} occupying an inversion center, there is no inversion center between the neighboring Co^{II} atoms within the chain. So both compounds show a weak ferromagnetic behavior. The canting angles γ at 2 K can be estimated through the equation $\sin(\gamma) = M_r/M_s$ (M_r obtained by extrapolating the high-field linear part of the magnetization curve at 2 K to zero field and $M_s = gS N\beta$, where $S = 3/2$ and g is obtained through the Curie constants) both up to 13° for **1·K** and **1·Cs**. The large canting angles of **1·K** and **1·Cs** are fewer in simple canted systems, which should be attributed not only to the strong Dzyaloshinsky–Moriya interaction but also to the strong single-ion magnetic anisotropy of Co^{II} ions and/or the axial magnetic anisotropy of chains.¹⁶ Moreover, strong frequency-dependent behaviors are both observed in the ac data of **1·K** and **1·Cs**. Since no structural disorder and no apparent magnetic frustration are found in **1·K** and **1·Cs**, these superparamagnetic dynamic relaxations are attached to be SCM-like behavior or magnetic domain-wall movement. The values of τ_0 and Δ/k_B in **1·K** and **1·Cs** are comparable with a few antiferromagnetic chains showing spin-canting and SCM behaviors reported in the literature.^{16a,17} However, the interchain magnetic exchanges, mediated by the alkali metals, organic ligands, or the π – π supramolecular interactions, cannot be ignored in these compounds, so the dynamic magnetic behaviors of **1·K** and **1·Cs** may come from the movement of the domain walls.^{18,19}

Conclusions

Two new 2D compounds based on mixed hydroxy/carboxylate-bridged Co^{II} chains have been synthesized by solvothermal reactions, in which the chains are well separated by alkali metal ions and pa ligands. With Cs^+ instead of K^+ , the intrachain,

- (14) (a) Morrish, A. H. *The Physical Principles of Magnetism*; Wiley: New York, 1966. (b) Mydosh, J. A. *Spin Glasses: An Experimental Introduction*; Taylor & Francis: London, 1993.
- (15) (a) Caneschi, A.; Gatteschi, D.; Lalioti, N.; Sangregorio, C.; Sessoli, R.; Venturi, G.; Vindigni, A.; Rettori, A.; Pini, M. G.; Novak, M. A. *Angew. Chem., Int. Ed.* **2001**, *40*, 1760. (b) Liu, T.-F.; Fu, D.; Gao, S.; Zhang, Y.-Z.; Sun, H.-L.; Su, G.; Liu, Y.-J. *J. Am. Chem. Soc.* **2003**, *125*, 13976.

- (16) (a) Bernot, K.; Luzon, J.; Sessoli, R.; Vindigni, A.; Thion, J.; Richeter, S.; Leclercq, D.; Larionova, J.; van der Lee, A. *J. Am. Chem. Soc.* **2008**, *130*, 1619. (b) Wang, X.-Y.; Wang, Z.-M.; Gao, S. *Inorg. Chem.* **2008**, *47*, 5720.
- (17) (a) Sun, Z.-M.; Prosvirin, A. V.; Zhao, H.-H.; Mao, J.-G.; Dunbar, K. R. *J. Appl. Phys.* **2005**, *97*, 3. (b) Pali, A. V.; Ostrovsky, S. M.; Klokishner, S. I.; Reu, O. S.; Sun, Z.-M.; Prosvirin, A. V.; Zhao, H.-H.; Mao, J.-G.; Dunbar, K. R. *J. Phys. Chem. A* **2006**, *110*, 14003.
- (18) Humphrey, S. M.; Alberola, A.; Gómez García, C. J.; Wood, P. T. *Chem. Commun.* **2006**, 1607.
- (19) (a) Zheng, L.-M.; Gao, S.; Yin, P.; Xin, X.-Q. *Inorg. Chem.* **2004**, *43*, 2151. (b) Liu, X.-T.; Wang, X.-Y.; Zhang, W.-X.; Cui, P.; Gao, S. *Adv. Mater.* **2006**, *18*, 2852.

interchain, and interlayer $\text{Co}^{\text{II}} \cdots \text{Co}^{\text{II}}$ distances are not significantly changed. Both compounds show spin canting antiferromagnetic behaviors with the critical temperature $T_c = 7$ K in **1•K** and 6 K in **1•Cs**. These two compounds are good examples for the magnetic studies on the chains of higher dimensional systems. More interestingly, superparamagnetic dynamic relaxations are observed for these simple chains with uniform antiferromagnetic interactions, which is scarce in the literature.^{16,18}

Acknowledgment. This work was supported by the “973 Project” (2007CB815302), NSFC (No. 20531070) and Science and Technology Department of Guangdong Province (No. 04205405).

Supporting Information Available: CIF files and additional structural plots, additional magnetic data, and the X-ray diffraction patterns (PDF). This material is available free of charge via the Internet at <http://pubs.acs.org>.

CM8012599